1997

Response of radiative fluxes to tiny random sea surface temperature disturbances

Chu, Peter C.

Chu, P.C., S.H. Lu, and Y.C. Chen, 1997: Response of radiative fluxes to tiny random sea surface temperature disturbances. Ninth Conference on Atmospheric Radiation, American

P1.28

RESPONSE OF RADIATIVE FLUXES TO TINY RANDOM SEA SURFACE TEMPERATURE DISTURBANCES

Peter C. Chu and Shihua Lu
Department of Oceanography, Naval Postgraduate School, Monterey, CA 93943

Tel: 408-656-3688, Fax: 408-656-3686, E-mail: chu@nps.navy.mil

1 Introduction

Much of the research (e.g., Namias, 1978; Douglas et al., 1982; Chervin et al., 1976; Kutzbach et al. 1977; Chervin et al., 1980) has been done on atmospheric response (including radiative response) to large or evident deterministic sea surface temperature (SST) anomalies at certain area of the ocean (e.g., mid-latitude North Pacific). In these studies, whether observational or modeling, the SST anomalies were of recognizable scale and always treated as deterministic functions of time and space. One might ask such a question: What is the radiative response to stochastic and tiny SST anomalies? Solving this problem has a great practical implication. If the radiative fluxes are not sensitive to small random SST change, we might use low resolution (in space and time) SST input to run the radiative module. If the radiative fluxes are very sensitive to tiny and random SST anomaly, we need use high quality and high resolution SST data. In this paper, we use the most recent version of the well-developed NCAR Community Climate Model Version 3 (CCM3) to explore the effects of tiny, random SST disturbance on the air-ocean surface fluxes.

2 Experimental Design

2.1 Model Description

The model that we used in this study is the NCAR Community Climate Model Version 3 (CCM3), which has evolved from the Australian spectral model described by Bourke et al. (1977) and McAvaney et al. (1978). CCM3 is the most recent version of the NCAR Community Climate Model. It should be noted that CCM3 has a drastic change to the previous version, CCM2, especially due to the addition of the Biosphere-Atmosphere Transfer Scheme (BATS) documented in Dickinson et al. (1993). CCM3 still uses the spectral transform method for the dynamic equations but uses a semi-Lagrangian method for transporting water (Rasch and Williamson, 1991). The model we used here contains 18 levels in the vertical with a top at 2.917 mb, and uses spherical harmonics as horizontal basis functions with a triangular truncation at wavenumber 21 (approximately a $5.6° \times 5.6°$ transform grid). The reader is referred to the foregoing articles for detailed description of the model physics (e.g., Kiehl 1990; Hack et al., 1993), apart from the radiative processes (e.g., Ramanathan et al., 1983; Briegleb, 1992; Slingo, 1989), atmospheric boundary layer processes (Troen and Mahrt, 1986; Holtslag et al., 1990), and mass flux scheme representing all types of moist convection (Hack, 1993).

2.2 A Tiny Gaussian-Type SST Anomaly

The Climate Analysis Center at NOAA/NWS/NMC is compiling an atlas containing monthly mean and anomalies of SST of global oceans. In January 1994 (Fig.1a), positive SST anomalies occupied vast areas of the Atlantic Ocean (both North and South) with anomalies of 2°C in the Gulf Stream extension just off the coast of North America, negative SST anomaly (minimum -3°C) was found. The SST anomaly has dipole patterns in both the Pacific Ocean (northern negative and southern positive) and the Indian Ocean (northern positive and southern negative). Anomaly reaches 1-2°C except off the west coast of North America where the maximum SST anomaly is greater than 3°C in July 1994 (Fig.1b).

In contrast to traditional studies, we use a Gaussian-type random variable (δT) to represent SST anomalies. The probability distribution function is given by

$$F(\delta T) = \frac{1}{\sqrt{2\pi}\sigma} \exp\left[-\frac{(\delta T)^2}{2\sigma^2}\right] \qquad (1)$$

where δT is a random variable with a zero mean and a standard deviation of σ. Since our interest is to see the response of atmosphere to tiny random SST anomalies,

we set

$$\sigma = 0.05°\text{C} \qquad (2)$$

in this study. This value (0.05°C) is less than the current instrumentation error. We used a random number generator (FORTRAN function, Ranf) to produce random disturbances for each grid point independently with mean value of zero and standard deviation of 0.05°C. Due to the nature of the Gaussian-type random distribution, we may find several points where the SST anomalies are 2-3 times of σ.

2.3 Experiments

2.3.1 Control Run

The initial condition used in this study is 1 September's climatology of the atmospheric and surface fields, which was provided by the NCAR Climate and Global Dynamics (CGD) Division. The surface boundary conditions were monthly sea and land surface temperatures (also obtained from NCAR CGD Division) linearly interpolated onto each time step (20 min). We integrated CCM3 for 16 months from 1 September to 31 December of the next year, and used the data between 1 January to 31 December of the second year for comparison.

2.3.2 Anomaly Run

After three months of the control run, we added a tiny Gaussian-type random SST anomaly with zero mean and 0.05°C standard deviation (for example as shown in Fig.1) generated by the FORTRAN random number generator applied to monthly SST data (first year December to second year December), and then interpolated into each time step. The rest of the forcing was kept the same. The model were integrated from 1 December of the first year to 31 December of the second year (Fig.2). We compare the air-ocean interfacial fluxes of momentum, heat, and moisture for the second year between the two runs, and call the difference between anomalous minus control runs as the anomaly response.

2.3.3 Root-Mean-Square Difference (RMSD)

The difference of the two runs (anomaly run minus control run) of any surface variable ψ is a function of space (x, y), and time t ,

$$\Delta\psi(x_i, y_j, t) = \psi_a(x_i, y_j, t) - \psi_c(x_i, y_j, t).$$

where ψ_a and ψ_c are the variables from anomaly and control runs, respectively. We define RMSD for investigating the temporal variation of the global difference,

$$RMSD_\psi(t) = \sqrt{\frac{1}{M}\sum_i\sum_j |\Delta(x_i, y_j, t)|^2} \qquad (3)$$

where M is the total number of horizontal grid points.

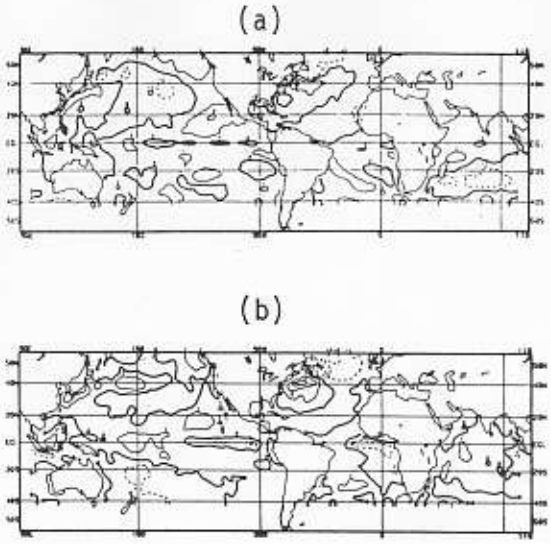

Figure 1 – Global SST anomaly (contour interval 1 degree C) from the NOAA/NWS/NMC Climate Analysis Center: (a) Januray 1994, and (b) July 1994.

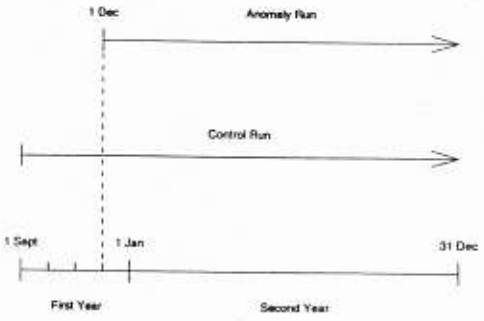

Figure 2 – Control and anomaly runs.

3 Statistical Test

The simulated fields in the two cases were analyzed in terms of monthly mean fields (near 30-day), from the second year January to December. The effect of tiny random SST anomaly on surface fluxes is presented by the difference between the two runs at each grid point. For statistical significance testing purposes, a normalized response is constructed using the procedures and estimates of the model's inherent variability from Chervin and Schneider (1976). That is, for each grid point of CCM3 a normalized response

$$r(x, y, t) = \frac{|\Delta\psi(x, y, t)|}{S_\psi(x, y, t)} \qquad (4)$$

is calculated for any variable (i.e., the tiny-random change response) at the grid point (x, y) and time period t, and $S_\psi(x, y, t)$ is the estimate of the standard deviation of monthly averages of the variable for the CCM3 control integration. This parameter, r, is proportional to t-statistic. It allows a potential assessment of the statistical significance of the change in model behavior, in this case, to a tiny random SST anomaly (Chervin et al., 1980.) Chervin and Schneider (1976) had shown that the sample value of t equals $r/\sqrt{2}$ at each grid point and there are four degrees of freedom. Table 1 (from Chervin, 1976) shows the relationship between r and the significant level for two-sided t-tests. The use of the two-sided t-test is based on the hypothesis that there is no specific signed difference, either positive or negative, in the response to the random SST anomaly. We begin with the usual null hypothesis that the means of the two runs are equal. The significance level is the probability that the given value of r is exceeded purely by chance. Equivalently , it is the probability of incorrectly rejecting the null hypothesis. As pointed by Chervin et al. (1980), we can regard as significant those response patterns which are associated with extensive regions where $r \geq 4$ (*a priori* significance criterion.) For clarity, in subsequent figures of surface flux response, we present the corresponding geographical distribution of r-values.

Since the added SST anomaly is a random variable, it is very hard to explain at the moment why there is strong surface flux response in certain areas. Therefore, in the subsequent sections we are concentrated more in describing the response.

r	Significance level for two-sided t-test
1	0.5169
2	0.2286
3	0.1002
4	0.0469
5	0.0238
6	0.0131
7	0.0077
8	0.0047
9	0.0031

Table 1. Significance levels for a selection of values of r corresponding to four degrees of freedom and t=r/sqrt(2) (from Chervin, 1976).

4 Monthly-Averaged Surface Radiative Budget of the Response

4.1 Short-Wave Radiation

The surface short-wave radiation anomaly (ΔR_S) response is shown in Fig.3a (for July) with the corresponding maps of the r-values being shown in Fig.3b (for July).

In July, five areas have evident response (Fig.3b): Tibetan Plateau ($r \simeq 10.3$), southeastern tip of Africa ($r \simeq 11.3$), eastern Australia ($r \simeq 5.4$), Gulf of California ($r \simeq 4.1$), and the northern Canada north of Arctic Circle ($r \simeq 4.6$). The surface short-wave radiative flux augments 106 W/m^2 over the Tibetan Plateau, 25 W/m^2 over the southeastern tip of Africa, and 42 W/m^2 over the eastern Australia, and 161 W/m^2 over the northern Canada north of Arctic Circle.

4.2 Long-Wave Radiation

The surface long-wave radiation anomaly (ΔR_L) response is shown in Fig.4a (for July) with the corresponding maps of the r-values being shown in Fig.4b (for July).

In July, four areas have evident response (Fig.4b): Tibetan Plateau ($r \simeq 8.5$), southeastern tip of Africa ($r \simeq 6.7$), eastern Australia ($r \simeq 5.0$), and southern tip of the Greenland Island ($r \simeq 4.8$). The surface short-wave radiative flux augments 63 W/m^2 over the Tibetan Plateau, 25 W/m^2 over the southeastern tip of Africa, and 46 W/m^2 in the eastern Australia, and reduces 43 W/m^2 near the southern tip of the Greenland Island.

5 Temporal Variations of RMSD

Temporal variation of RMSD (measure of the global response) for various surface heat fluxes is shown in Fig.5. Similar to the surface wind stress, two modes were found

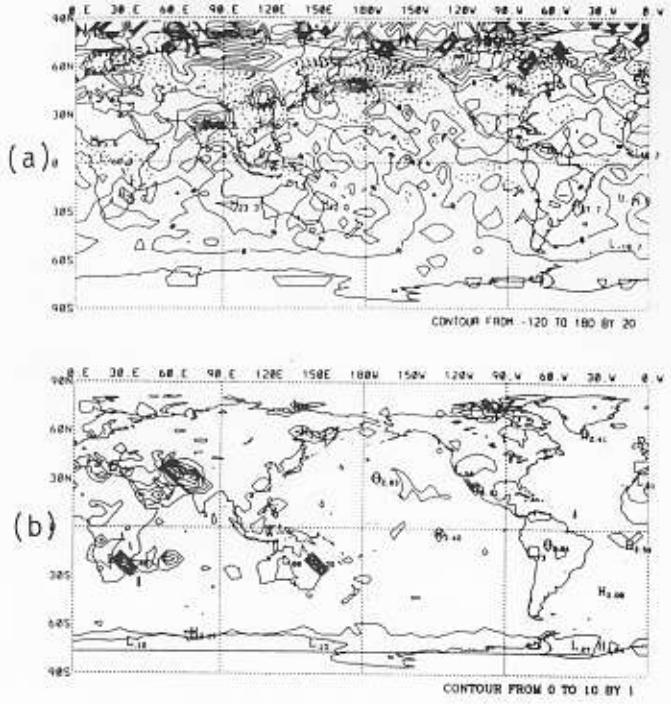

Figure 3 – (a) Response of monthly averaged July surface short wave radiation (W/m2) to a tiny random SST anomaly, and (b) the r-statistics.**

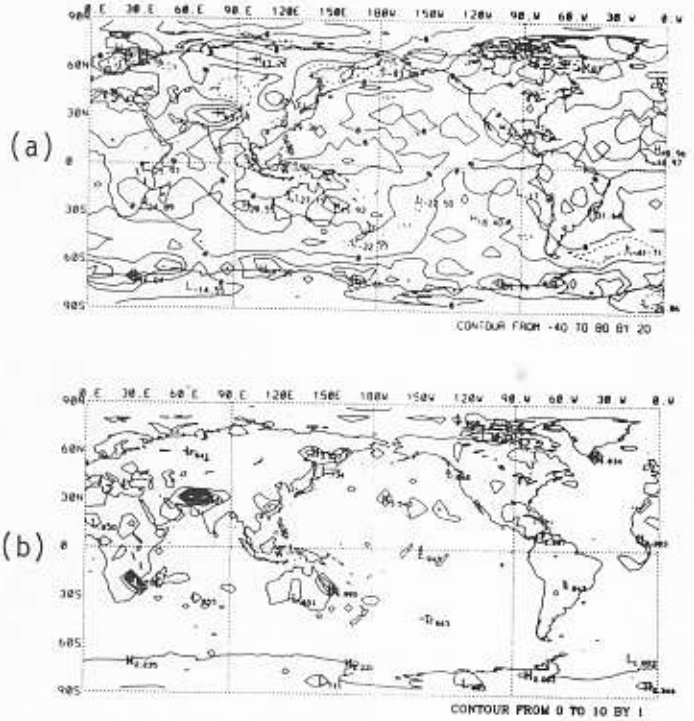

Figure 4 – Same as in Fig.3 except for monthly averaged July surface long wave radiation (W/m2).**

from Fig.5: (a) near-linearly growing mode and (b) oscillatory mode. During the near-linearly growing modes, the RMSDs increases from 0 to evident values at around the 20-th day:

$$RMSD_{R_S} \simeq 70 W/m^2, \quad RMSD_{R_L} \simeq 42 W/m^2,$$

During the oscillatory modes, RMSD_{R_S} oscillates between 76 W/m^2 and 49 W/m^2; RMSD_{R_L} oscillates between 43 W/m^2 and 33 W/m.

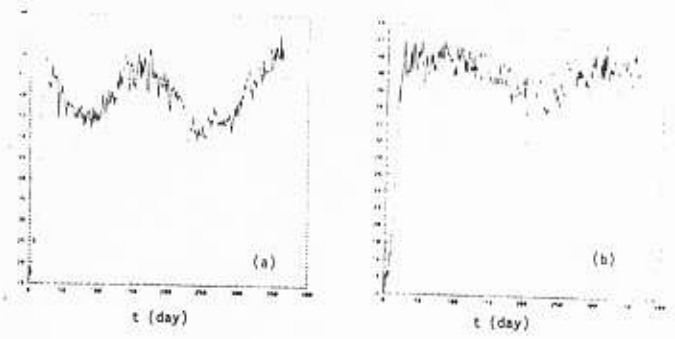

Figure 5 – Temporal variation of RMSD for surface radiative fluxes (unit: W/m2): (a) solar radiation and (b) long-wave radiation.The horizontal axis t=0 indicates the first day when the tiny random SST anomaly was introduced.**

6 Conclusions

1. This study shows large responses of surface radiative fluxes to a tiny Gaussian-type random SST disturbance. After three months of the control run of the NCAR CCM3 model, we introduced a tiny Gaussian-type random SST anomaly (zero mean and 0.05°C standard deviation) generated by a FORTRAN random number generator to the SST data at each grid and ran the model for another 13 months (anomaly run). The rest of the forcing were kept the same as the control run. The monthly mean values for both the control and anomaly runs were used for comparison. It is quite surprising that the responses of surface fluxes were very strong, even in the monthly mean values.

2. The maximum surface flux responses are found as: 161 W/m^2 for $|\Delta R_S|$, and 63 W/m^2 for $|\Delta R_L|$.

3. Two modes of the global response were found in this study: (a) near-linearly growing mode and (b) oscillatory mode. During the near-linearly growing modes, the **difference of the root-mean-squares** (RMSDs) increase from 0 to evident values at around the 20-th day:

$$RMSD_{R_S} \simeq 70 W/m^2, \quad RMSD_{R_L} \simeq 42 W/m^2,$$

During the oscillatory modes, RMSDs oscillates around these evident values.

4. Several geographic locations were found sensitive to the tiny-SST anomalies: Polar regions, Tibetan Plateau, Northeast Australia, North Africa, South tip of the Africa, and western Pacific.

5. Integration of atmospheric model needs accurate SST data. The noise in the SST data may bring drastic change in the model results.

6. From the RMSD values, we estimate that the uncertainty of 70 W/m^2 in the surface radiative flux.

7 ACKNOWLEDGMENTS

Authors are grateful to Yongfu Qian, Laura Ehret, and Qianqian Wang for invaluable comments. This research is sponsored by the Office of Naval Research (ONR) Naval Ocean Modeling Program (NOMP), High Latitude (HL) Program, and the Naval Postgraduate School.

REFERENCES

Bourke, W., B. McAvanney, K. Puri, and R. Thurling, Global modeling of atmospheric flow by spectral methods, **Methods in Computational Physics,** 17, General Circulation Models of the Atmosphere, J. Chang, Ed., Academic Press, 267-324, 1977.

Briegleb, B.D., Delta-Eddington approximation for solar radiation in the NCAR Community Climate Model, **J. Geophys. Res.,** 97, 7603-7612, 1992.

Chervin, R.M., W.M. Washington and S.H. Schneider, Testing the statistical significance of the response of the NCAR general circulation model to North Pacific Ocean surface temperature anomalies, **J. Atmos. Sci.,** 33, 413-423, 1976.

Chervin, R.M., J.E. Kutzbach, D.D. Houghton and R.G. Gallimore, Response of the NCAR general circulation model to prescribed changes in ocean surface temperature. Part II: Midlatitude and subtropical changes, **J. Atmos. Sci.,** 37, 308-332, 1980.

Davis, R.E., Predictability of sea surface temperature and sea level pressure anomalies over the North Pacific Ocean, **J. Phys. Oceanogr.,** 6, 249-266, 1976

Dickinson R.E., A. Herderson-Sellers, and P.J. Kennedy, Biosphere-Atmosphere Transfer Scheme (BATS) Version 1e as coupled to the NCAR Community Climate Model, **NCAR Technical Note,** 1993.

Douglas, A.V., D.R. Cayan, and J. Namias, Large-scale changes in North Pacific and North American weather patterns in recent decades, **Mon. Wea. Rev.,** 110, 1851-1862, 1982.

Hack, J.J., B.A. Boville, B.P. Briegleb, J.T. Kiehl, P.J. Rasch, and D.L. Williamson, Description of the NCAR Community Climate Model (CCM2), **NCAR Technical Note,** NCAR/TN-382+STR, 1993.

Holtslag, E.I., F. de Bruijn, and H.-L. Pan, A high resolution air mass transformation model for short-range weather forecasting. **Mon. Wea. Rev.,** 118, 1561-1575, 1990.

Kiehl, J.T., Modeling and validation of clouds and radiation in the NCAR Community Climate Model, **Proc. ECMWF/WCRP Workshop on Clouds, Radiative Transfer and Hydrological Cycle,** 413-450, Reading, 12-15 November 1990.

Kutzbach, J.E., R.M. Chervin and D.D. Houghton, Response of the NCAR general circulation model to prescribed changes in ocean surface temperature Part I: Mid-latitude changes, **J. Atmos. Sci.,** 34, 1200-1213, 1977.

McAvaney, B.J., W. Bourke and K. Puri, A global spectral model for simulation of the general circulation, **J. Atmos. Sci.,** 35, 1557-1583, 1978.

Namias, J., Multiple causes of the North American abnormal winter 1976-77, **Mon. Wea. Rev.,** 106, 279-295, 1978.

NMC, **Climate Diagnostics Bulletins,** Climate Prediction Center, 1995

Ramanathan, V., E.J. Pitcher, R.C., Malone and M.L. Blackmon, The response of a spectral general circulation model to refinements in radiative processes, **J. Atmos. Sci.,** 40, 605-630, 1983.

Rasch, P.J. and D.L. Williamson, The sensitivity of a general circulation model climate to the moisture transport formulation, **J. Geophys. Res.,** 96, 13,123-13,137, 1991.

Slingo, A., A GCM parameterization for the shortwave radiative properties of water clouds, **J. Atmos. Sci.,** 46, 1419-1427, 1989.